



Received 4 April 2019

Accepted 22 May 2019

Edited by J. T. Mague, Tulane University, USA

Keywords: crystal structure; quinoline; offset π – π interactions; Hirshfeld surface analysis; DFT.**CCDC reference:** 1890687**Supporting information:** this article has supporting information at journals.iucr.org/e

Crystal structure, DFT study and Hirshfeld surface analysis of ethyl 6-chloro-2-ethoxyquinoline-4-carboxylate

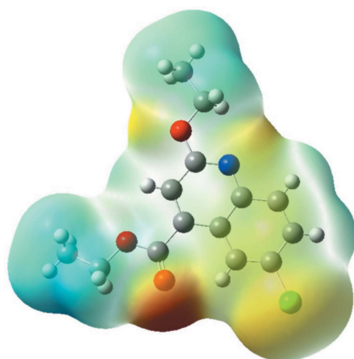
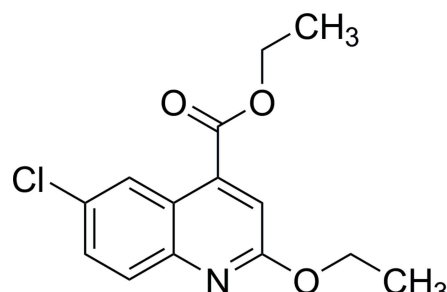
Younos Bouzian,^{a*} Khalid Karrouchi,^b El Hassane Anouar,^c Rachid Bouhfid,^d Suhana Arshad^e and El Mokhtar Essassi^a

^aLaboratory of Heterocyclic Organic Chemistry, URAC 21, Pole of Competence, Pharmacocchemistry, Av Ibn Battouta, BP 1014, Faculty of Sciences, Mohammed V University, Rabat, Morocco, ^bLaboratory of Plant Chemistry, Organic and Bioorganic Synthesis, URAC23, Faculty of Science, BP 1014, GEOPAC Research Center, Mohammed V University, Rabat, Morocco, ^cDepartment of Chemistry, College of Science and Humanities, Prince Sattam Bin Abdulaziz University, PO Box 830, Al Kharj, Saudi Arabia, ^dMoroccan Foundation for Advanced Science, Innovation and Research (MASCIR), Rabat, Morocco, and ^eX-ray Crystallography Unit, School of Physics, Universiti Sains Malaysia, 11800 USM, Penang, Malaysia. *Correspondence e-mail: younos.bouzian19@gmail.com

In the title quinoline derivative, $C_{14}H_{14}ClNO_3$, there is an intramolecular C—H···O hydrogen bond forming an $S(6)$ graph-set motif. The molecule is essentially planar with the mean plane of the ethyl acetate group making a dihedral angle of $5.02(3)^\circ$ with the ethyl 6-chloro-2-ethoxyquinoline mean plane. In the crystal, offset π – π interactions with a centroid-to-centroid distance of $3.4731(14)$ Å link inversion-related molecules into columns along the c -axis direction. Hirshfeld surface analysis indicates that H···H contacts make the largest contribution (50.8%) to the Hirshfeld surface.

1. Chemical context

Quinoline derivatives represent an important class of bioactive heterocyclic compounds in the field of pharmaceuticals (Chu *et al.*, 2019). Quinoline derivatives possess various pharmacological properties such as antibacterial (Panda *et al.*, 2015), anti-HCV (Cannalire *et al.*, 2016), antiviral (Sekgota *et al.*, 2017), anticancer (Tang *et al.*, 2018), antimalarial (van Heerden *et al.*, 2012), antileishmanial (Palit *et al.*, 2009), antitubecular (Xu *et al.*, 2017), anti-inflammatory (de Santos *et al.*, 2015) and anti-Alzheimer's (Bolognesi *et al.*, 2007) activities. The present work is a continuation of our research work devoted to the synthesis and crystal structure of heterocyclic derivatives (Bouzian *et al.*, 2018; Chkirate *et al.* 2019*a,b*). As part of our studies in this area, we prepared the title compound by reacting ethyl 6-chloro-2-oxo-1,2-dihydro-quinoline-4-carboxylate with bromoethane in the presence of a catalytic quantity of tetra-*n*-butylammonium bromide. We report herein on its crystal and molecular structures along with the Hirshfeld surface analysis.



OPEN ACCESS

Table 1
Hydrogen-bond geometry (\AA , $^\circ$).

$D-\text{H}\cdots A$	$D-\text{H}$	$\text{H}\cdots A$	$D\cdots A$	$D-\text{H}\cdots A$
C5—H5A···O3	0.93	2.24	2.872 (4)	125

2. Structural commentary

The molecular structure of the title compound is shown in Fig. 1a. The molecule consists of a quinoline fused-ring system (N1/C1–C9) with methoxyethane (O2/C10/C11), ethyl acetate (O3/O4/C13/C14) and a chlorine atom (Cl1) substituents. The intramolecular C5—H5A···O3 hydrogen bond (Table 1) forms an $S(6)$ graph-set motif, stabilizing the molecular structure and preventing free rotation between the 6-chloroquinoline ring (Cl1/N1/C1–C9) and the ethyl acetate (O3/O4/C12–C14) moiety. Additionally, the presence of this intramolecular C—H···O interaction leads to an essentially planar molecular structure (Fig. 1b), where the ethyl acetate (O3/O4/C12–C14) mean plane is twisted slightly at a dihedral angle of $5.02 (3)^\circ$ with respect to the mean plane of the ethyl 6-chloro-2-ethoxyquinoline (Cl1/O2/C1–C11) moiety. This essentially planar molecular structure may be considered an important binding mode that can enhance biological activity (Bierbach *et al.*, 1999).

3. Supramolecular features

In the crystal, molecules lie in a plane parallel to the $(10\bar{2})$ crystallographic plane (Fig. 2a). They are linked by offset $\pi\cdots\pi$ interactions (Fig. 2b) involving inversion-related pyridine rings. These interactions link the molecules into columns up

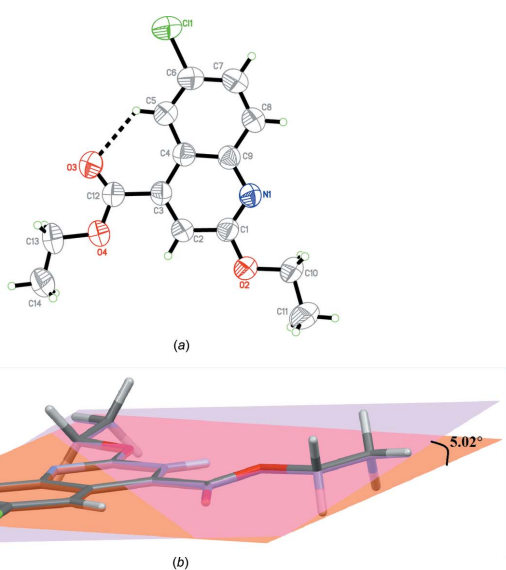


Figure 1

(a) The molecular structure of the title compound, with the atom labelling and displacement ellipsoids drawn at the 50% probability level. The dashed line represents the intramolecular C—H···O interaction (Table 1). (b) The essentially planar structure of the title compound.

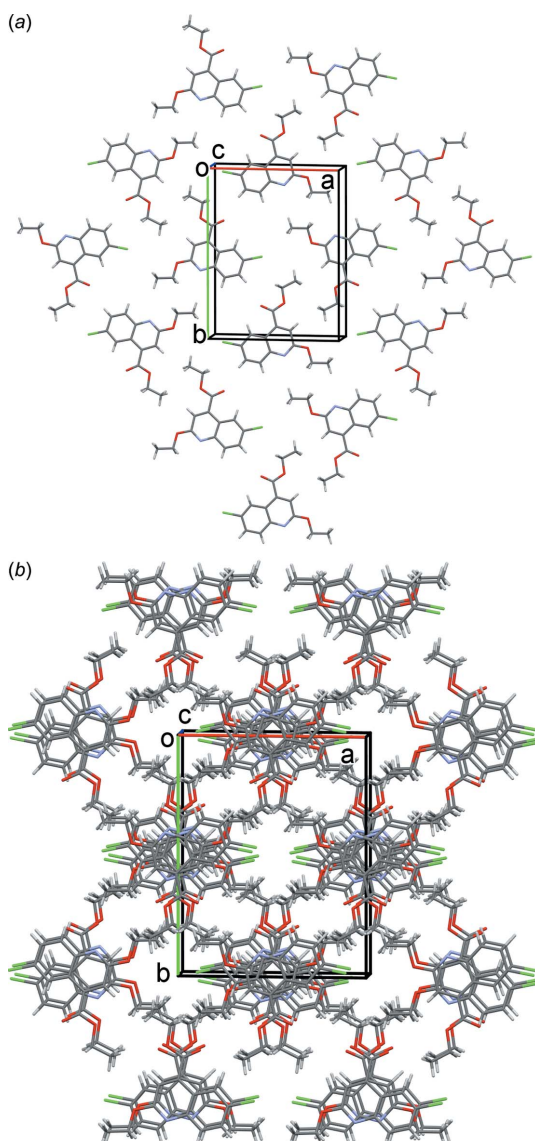


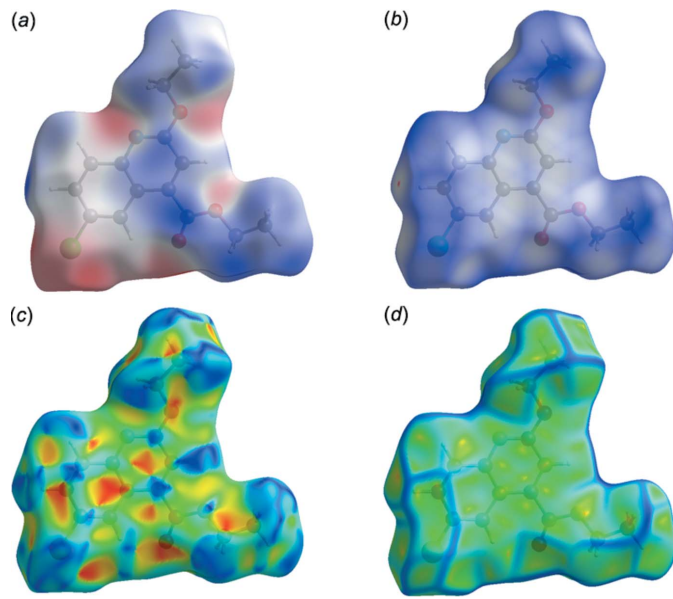
Figure 2

(a) A partial view along the c axis of the crystal packing of the title compound. (b) A view along the c axis of the crystal packing of the title compound.

the c -axis direction with a centroid-to-centroid ($Cg\cdots Cg^i$) distance of $3.4731 (14)$ \AA [Cg is centroid of the N1/C1–C4/C9 ring, interplanar distance = $3.397 (1)$ \AA , offset = 0.722 \AA ; symmetry code (i): $-x + 1, -y, -z + 1$].

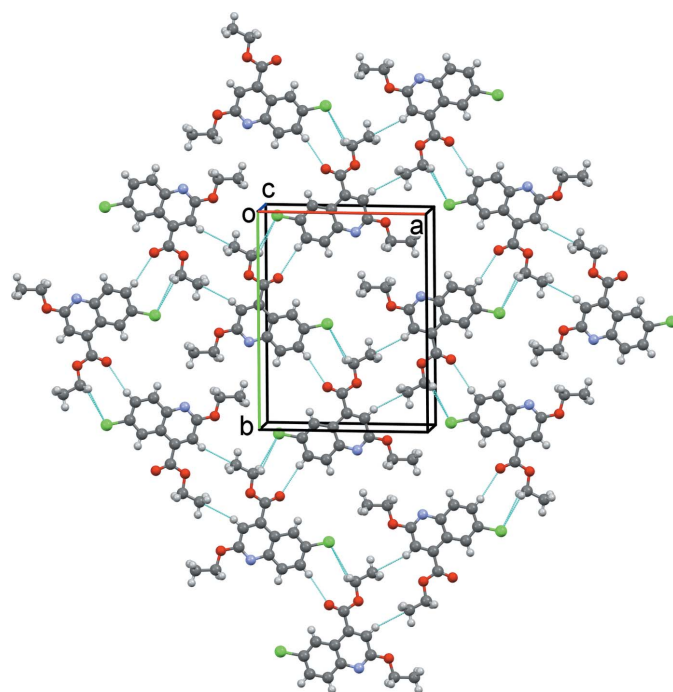
4. Hirshfeld surface analysis

The Hirshfeld surface analysis (Spackman & Jayatilaka, 2009) and the associated two-dimensional fingerprint plots (McKinnon *et al.*, 2007) were performed with *Crystal-Explorer17* (Turner *et al.*, 2017). Internal and external (d_i and d_e) contact distances from the Hirshfeld surface to the nearest atom inside and outside enables the analysis of the intermolecular interactions through the mapping of d_{norm} . The Hirshfeld surfaces (HS) mapped over the electrostatic potential (-0.0534 to 0.0319 atomic units) and d_{norm} (-0.0210

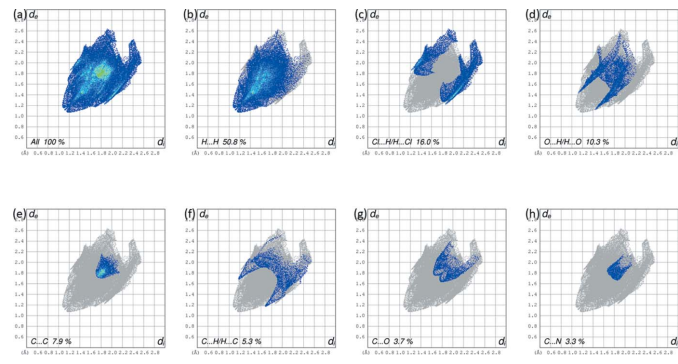
**Figure 3**

Hirshfeld surface of the title compound mapped over: (a) electrostatic potential, (b) d_{norm} , (c) shape-index and (d) curvedness.

to 1.4779 arbitrary units) are shown in Fig. 3a and 3b. The red spots on the Hirshfeld surface indicate interactions involved in $\text{H}\cdots\text{O}$ contacts. The $\pi\cdots\pi$ stacking is confirmed by the small blue regions surrounding bright red spots in the aromatic ring in Fig. 3c, the Hirshfeld surface mapped over the shape-index, and by the flat regions around the aromatic regions in Fig. 3d, the Hirshfeld surface mapped over the curvedness.

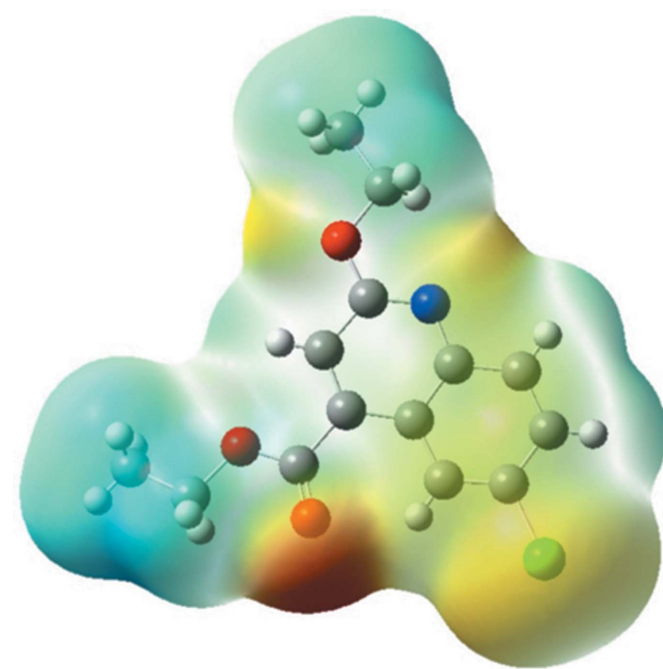
**Figure 4**

A view of the intermolecular contacts (dashed lines) in the crystal of the title compound. They are all longer by 0.02 Å than the sum of the van der Waals radii of the individual atoms.

**Figure 5**

(a) The two-dimensional fingerprint plot of the title compound, and the fingerprint plots delineated into: (b) $\text{H}\cdots\text{H}$ (50.8%), (c) $\text{Cl}\cdots\text{H}/\text{H}\cdots\text{Cl}$ (16.0%), (d) $\text{O}\cdots\text{H}/\text{H}\cdots\text{O}$ (10.3%), (e) $\text{C}\cdots\text{C}$ (7.9%), (f) $\text{C}\cdots\text{H}/\text{H}\cdots\text{C}$ (5.3%), (g) $\text{C}\cdots\text{O}$ (3.7%) and (h) $\text{C}\cdots\text{N}$ (3.3%) contacts.

There are no significant classical intermolecular contacts present in the crystal according to the analysis of the crystal structure using *PLATON* (Spek, 2009). However, from the Hirshfeld surface analysis and the two-dimensional fingerprint plots it can be seen that $\text{H}\cdots\text{H}$, $\text{C}\cdots\text{H}$, $\text{Cl}\cdots\text{H}$ and $\text{O}\cdots\text{H}$ contacts (Fig. 4) contribute to the cohesion of the crystal structure. The two-dimensional fingerprint plots are given in Fig. 5. The two-dimensional fingerprint of the (d_i , d_e) points associated with the hydrogen atoms is shown in Fig. 5b. It is characterized by an end point that points to the origin, indicating the presence of the $\text{H}\cdots\text{H}$ contacts that contribution 50.8%. The $\text{Cl}\cdots\text{H}/\text{H}\cdots\text{Cl}$ contacts between the chlorine atoms inside the Hirshfeld surface and the hydrogen atoms outside the surface and *vice versa* contribute 16.0% (Fig. 5c).

**Figure 6**

EPS of the title compound obtained at the B3LYP/6-31+G(d,p) level of theory.

Table 2
Experimental details.

Crystal data	
Chemical formula	C ₁₄ H ₁₄ ClNO ₃
M _r	279.71
Crystal system, space group	Monoclinic, C2/c
Temperature (K)	296
a, b, c (Å)	14.2634 (7), 16.0124 (7), 13.7732 (6)
β (°)	117.748 (2)
V (Å ³)	2783.9 (2)
Z	8
Radiation type	Mo Kα
μ (mm ⁻¹)	0.28
Crystal size (mm)	0.50 × 0.47 × 0.37
Data collection	
Diffractometer	Bruker SMART APEXII DUO CCD area-detector
Absorption correction	Multi-scan (SADABS; Bruker, 2009)
No. of measured, independent and observed [I > 2σ(I)] reflections	45458, 3190, 2228
R _{int}	0.029
(sin θ/λ) _{max} (Å ⁻¹)	0.650
Refinement	
R[F ² > 2σ(F ²)], wR(F ²), S	0.058, 0.203, 1.10
No. of reflections	3190
No. of parameters	174
H-atom treatment	H-atom parameters constrained
Δρ _{max} , Δρ _{min} (e Å ⁻³)	0.30, -0.32

Computer programs: *APEX2* and *SAINT* (Bruker, 2009), *SHELXS* and *SHELXTL* (Sheldrick, 2008), *SHELXL2014* (Sheldrick, 2015), *Mercury* (Macrae *et al.*, 2008) and *PLATON* (Spek, 2009).

The O···H/H···O (10.3%) plot shows two symmetrical wings on the left and right sides (Fig. 5d). The C···C contacts contribute 7.9% (Fig. 5e), the C···H/H···C contacts contribute 5.3% (Fig. 5e), followed by the C···O contacts at 3.7% (Fig. 5g) and the C···N contacts at 3.3% (Fig. 3h).

5. DFT study

The electrostatic potential surface (ESP) was also calculated using DFT methods at the B3LYP/6-311+G(d,p) level of theory using the *Gaussian 09* package (Frisch *et al.*, 2009). The negative region on the electrostatic potential appears in red and corresponds to hydrogen-bond acceptors, while the positive region of electrostatic potential appears in blue and corresponds to hydrogen-bond donors (Fig. 6).

6. Database survey

A search of the Cambridge Structural Database (CSD, Version 5.40, last update May 2019; Groom *et al.*, 2016) for the 6-chloroquinoline skeleton gave 100 hits, including 6-chloroquinoline itself (CSD refcode CLQUIN; Merlino, 1968). Only a limited number of these structures are similar to the title compound. There are no compounds with a 6-chloro-2-ethoxyquinoline moiety and only four compounds with a 6-chloro-2-methoxyquinoline moiety. These include, 1-{6-chloro-2-[{(2-chloro-8-methylquinolin-3-yl)methoxy]-4-phenylquinolin-3-yl}ethanone (DUVJEK; Khan *et al.*, 2010a), ethyl 6-chloro-2-[(2-chloro-7,8-dimethylquinolin-3-yl)methoxy]-4-phenylquinoline-3-carboxylate (KUVFEN; Khan *et al.*, 2010b), 1-{6-chloro-2-[(2-chloroquinolin-3-yl)methoxy]-4-phenylquinolin-3-yl}ethanone (YUQTAG; Khan *et al.*, 2010c), and 1-{6-chloro-2-[(2-chloro-6-methylquinolin-3-yl)methoxy]-4-phenylquinolin-3-yl}ethanone (YUQVIQ; Khan *et al.*, 2010d). Two other relevant compounds with an ethyl carboxylate substituent include ethyl 2,6-dichloro-4-phenylquinoline-3-carboxylate (DUKKUQ; Roopan *et al.*, 2009) and ethyl 6-chloro-2-methyl-4-phenylquinoline-3-carboxylate (DUKJEZ; Subashini *et al.*, 2009). In the crystals of all of the above mentioned compounds, molecules are linked by offset π-π interactions involving inversion-related quinoline units.

ylquinolin-3-yl}ethanone (DUVJEK; Khan *et al.*, 2010a), ethyl 6-chloro-2-[(2-chloro-7,8-dimethylquinolin-3-yl)methoxy]-4-phenylquinoline-3-carboxylate (KUVFEN; Khan *et al.*, 2010b), 1-{6-chloro-2-[(2-chloroquinolin-3-yl)methoxy]-4-phenylquinolin-3-yl}ethanone (YUQTAG; Khan *et al.*, 2010c), and 1-{6-chloro-2-[(2-chloro-6-methylquinolin-3-yl)methoxy]-4-phenylquinolin-3-yl}ethanone (YUQVIQ; Khan *et al.*, 2010d). Two other relevant compounds with an ethyl carboxylate substituent include ethyl 2,6-dichloro-4-phenylquinoline-3-carboxylate (DUKKUQ; Roopan *et al.*, 2009) and ethyl 6-chloro-2-methyl-4-phenylquinoline-3-carboxylate (DUKJEZ; Subashini *et al.*, 2009). In the crystals of all of the above mentioned compounds, molecules are linked by offset π-π interactions involving inversion-related quinoline units.

7. Synthesis and crystallization

A solution of 0.5 g (1.99 mmol) of ethyl 6-chloro-2-oxo-1,2-dihydroquinoline-4-carboxylate in 25 ml of DMF was mixed with 0.3 ml (3.98 mmol) of bromoethane, 0.55 g (3.98 mmol) of K₂CO₃ and 0.06 g (0.199 mmol) of tetra-*n*-butylammonium bromide (TBAB). The reaction mixture was stirred at room temperature in DMF for 24 h. After removal of salts by filtration, the DMF was evaporated under reduced pressure and the residue obtained was dissolved in dichloromethane. The organic phase was dried over Na₂SO₄ then concentrated *in vacuo*. The resulting mixture was chromatographed on a silica gel column [eluent: ethyl acetate/hexane (1:9 v/v)]. Colourless crystals were obtained when the solvent was allowed to evaporate (yield: 32%).

8. Refinement

Crystal data, data collection and structure refinement details are summarized in Table 2. All H atoms were positioned geometrically and refined using a riding model: C—H = 0.93–0.97 Å with U_{iso}(H) = 1.5U_{eq}(C-methyl) and 1.2U_{eq}(C) for other H atoms. A rotating group model was applied to the methyl groups.

Funding information

This project was supported by the Deanship of Scientific Research at Prince Sattam Bin Abdulaziz University under research project No. 2017/01/7199.

References

- Bierbach, U., Qu, Y., Hambley, T. W., Peroutka, J., Nguyen, H. L., Doegee, M. & Farrell, N. (1999). *Inorg. Chem.* **38**, 3535–3542.
- Bolognesi, M. L., Cavalli, A., Valgimigli, L., Bartolini, M., Rosini, M., Andrisano, V., Recanatini, M. & Melchiorre, C. (2007). *J. Med. Chem.* **50**, 6446–6449.
- Bouzian, Y., Hlimi, F., Sebbar, N. K., El Hafi, M., Hni, B., Essassi, E. M. & Mague, J. T. (2018). *IUCrData*, **3**, x181438.
- Bruker (2009). *APEX2*, *SAINT* and *SADABS*. Bruker AXS Inc., Madison, Wisconsin, USA.
- Cannalire, R., Barreca, M. L., Manfroni, G. & Cecchetti, V. (2016). *J. Med. Chem.* **59**, 16–41.

- Chkirate, K., Kansiz, S., Karrouchi, K., Mague, J. T., Dege, N. & Essassi, E. M. (2019a). *Acta Cryst. E***75**, 33–37.
- Chkirate, K., Kansiz, S., Karrouchi, K., Mague, J. T., Dege, N. & Essassi, E. M. (2019b). *Acta Cryst. E***75**, 154–158.
- Chu, X. M., Wang, C., Liu, W., Liang, L. L., Gong, K. K., Zhao, C. Y. & Sun, K. L. (2019). *Eur. J. Med. Chem.* **161**, 101–117.
- Frisch, M. J., et al. (2009). Gaussian 09. Gaussian, Inc., Wallingford CT, USA.
- Groom, C. R., Bruno, I. J., Lightfoot, M. P. & Ward, S. C. (2016). *Acta Cryst. B***72**, 171–179.
- Heerden, L. van, Cloete, T. T., Breytenbach, J. W., de Kock, C., Smith, P. J., Breytenbach, J. C. & N'Da, D. D. (2012). *Eur. J. Med. Chem.* **55**, 335–345.
- Khan, F. N., Hathwar, V. R., Kumar, R., Kumar, A. S. & Akkurt, M. (2010a). *Acta Cryst. E***66**, o1930.
- Khan, F. N., Hathwar, V. R., Kumar, R., Kushwaha, A. K. & Akkurt, M. (2010d). *Acta Cryst. E***66**, o1693–o1694.
- Khan, F. N., Roopan, S. M., Hathwar, V. R. & Akkurt, M. (2010b). *Acta Cryst. E***66**, o972–o973.
- Khan, F. N., Roopan, S. M., Kumar, R., Hathwar, V. R. & Akkurt, M. (2010c). *Acta Cryst. E***66**, o1607–o1608.
- Macrae, C. F., Bruno, I. J., Chisholm, J. A., Edgington, P. R., McCabe, P., Pidcock, E., Rodriguez-Monge, L., Taylor, R., van de Streek, J. & Wood, P. A. (2008). *J. Appl. Cryst.* **41**, 466–470.
- McKinnon, J. J., Jayatilaka, D. & Spackman, M. A. (2007). *Chem. Commun.* pp. 3814–3816.
- Merlino, S. (1968). *Atti Accad. Naz. Lincei*, **45**, 147.
- Palit, P., Paira, P., Hazra, A., Banerjee, S., Gupta, A. D., Dastidar, S. G. & Mondal, N. B. (2009). *Eur. J. Med. Chem.* **44**, 845–853.
- Panda, S. S., Liaqat, S., Girgis, A. S., Samir, A., Hall, C. D. & Katritzky, A. R. (2015). *Bioorg. Med. Chem. Lett.* **25**, 3816–3821.
- Roopan, S. M., Khan, F. N., Vijetha, M., Hathwar, V. R. & Ng, S. W. (2009). *Acta Cryst. E***65**, o2982.
- Santos, R. M. de, Barros, P. R., Bortoluzzi, J. H., Meneghetti, M. R., da Silva, Y. K. C., da Silva, A. E., da Silva Santos, M. & Alexandre-Moreira, M. S. (2015). *Bioorg. Med. Chem.* **23**, 4390–4396.
- Sekgota, K. C., Majumder, S., Isaacs, M., Mnkandhla, D., Hoppe, H. C., Khanye, S. D., Kriel, F. H., Coates, J. & Kaye, P. T. (2017). *Bioorg. Chem.* **75**, 310–316.
- Sheldrick, G. M. (2008). *Acta Cryst. A***64**, 112–122.
- Sheldrick, G. M. (2015). *Acta Cryst. C***71**, 3–8.
- Spackman, M. A. & Jayatilaka, D. (2009). *CrystEngComm*, **11**, 19–32.
- Spek, A. L. (2009). *Acta Cryst. D***65**, 148–155.
- Subashini, R., Khan, F. N., Mittal, S., Hathwar, V. R. & Ng, S. W. (2009). *Acta Cryst. E***65**, o2986.
- Tang, Q. D., Duan, Y. L., Xiong, H. H., Chen, T., Xiao, Z., Wang, L. X., Xiao, Y. Y., Huang, S. M., Xiong, Y., Zhu, W., Gong, P. & Zheng, P. (2018). *Eur. J. Med. Chem.* **158**, 201–213.
- Turner, M. J., McKinnon, J. J., Wolff, S. K., Grimwood, D. J., Spackman, P. R., Jayatilaka, D. & Spackman, M. A. (2017). *CrystalExplorer17*. University of Western Australia. <http://hirshfeldsurface.net>
- Xu, Z., Gao, C., Ren, Q. C., Song, X. F., Feng, L. S. & Lv, Z. S. (2017). *Eur. J. Med. Chem.* **139**, 429–440.

supporting information

Acta Cryst. (2019). E75, 912-916 [https://doi.org/10.1107/S2056989019007473]

Crystal structure, DFT study and Hirshfeld surface analysis of ethyl 6-chloro-2-ethoxyquinoline-4-carboxylate

Younos Bouzian, Khalid Karrouchi, El Hassane Anouar, Rachid Bouhfid, Suhana Arshad and El Mokhtar Essassi

Computing details

Data collection: *APEX2* (Bruker, 2009); cell refinement: *SAINT* (Bruker, 2009); data reduction: *SAINT* (Bruker, 2009); program(s) used to solve structure: *SHELXS* (Sheldrick, 2008); program(s) used to refine structure: *SHELXL2014* (Sheldrick, 2015); molecular graphics: *SHELXTL* (Sheldrick, 2008) and *Mercury* (Macrae *et al.*, 2008); software used to prepare material for publication: *SHELXTL* (Sheldrick, 2008) and *PLATON* (Spek, 2009).

Ethyl 6-chloro-2-ethoxyquinoline-4-carboxylate

Crystal data

$C_{14}H_{14}ClNO_3$
 $M_r = 279.71$
Monoclinic, $C2/c$
 $a = 14.2634 (7)$ Å
 $b = 16.0124 (7)$ Å
 $c = 13.7732 (6)$ Å
 $\beta = 117.748 (2)^\circ$
 $V = 2783.9 (2)$ Å³
 $Z = 8$

$F(000) = 1168$
 $D_x = 1.335 \text{ Mg m}^{-3}$
Mo $K\alpha$ radiation, $\lambda = 0.71073$ Å
Cell parameters from 9928 reflections
 $\theta = 2.5\text{--}24.5^\circ$
 $\mu = 0.28 \text{ mm}^{-1}$
 $T = 296 \text{ K}$
Block, colourless
 $0.50 \times 0.47 \times 0.37 \text{ mm}$

Data collection

Bruker SMART APEXII DUO CCD area-detector diffractometer
Radiation source: fine-focus sealed tube
 φ and ω scans
Absorption correction: multi-scan (*SADABS*; Bruker, 2009)

45458 measured reflections
3190 independent reflections
2228 reflections with $I > 2\sigma(I)$
 $R_{\text{int}} = 0.029$
 $\theta_{\text{max}} = 27.5^\circ, \theta_{\text{min}} = 2.1^\circ$
 $h = -18 \rightarrow 18$
 $k = -20 \rightarrow 20$
 $l = -17 \rightarrow 17$

Refinement

Refinement on F^2
Least-squares matrix: full
 $R[F^2 > 2\sigma(F^2)] = 0.058$
 $wR(F^2) = 0.203$
 $S = 1.10$
3190 reflections
174 parameters
0 restraints

Primary atom site location: structure-invariant direct methods
Secondary atom site location: difference Fourier map
Hydrogen site location: inferred from neighbouring sites
H-atom parameters constrained

$$w = 1/[\sigma^2(F_o^2) + (0.0854P)^2 + 2.5795P]$$

where $P = (F_o^2 + 2F_c^2)/3$
 $(\Delta/\sigma)_{\max} < 0.001$

$$\Delta\rho_{\max} = 0.30 \text{ e } \text{\AA}^{-3}$$

$$\Delta\rho_{\min} = -0.32 \text{ e } \text{\AA}^{-3}$$

Special details

Geometry. All esds (except the esd in the dihedral angle between two l.s. planes) are estimated using the full covariance matrix. The cell esds are taken into account individually in the estimation of esds in distances, angles and torsion angles; correlations between esds in cell parameters are only used when they are defined by crystal symmetry. An approximate (isotropic) treatment of cell esds is used for estimating esds involving l.s. planes.

Fractional atomic coordinates and isotropic or equivalent isotropic displacement parameters (\AA^2)

	<i>x</i>	<i>y</i>	<i>z</i>	$U_{\text{iso}}^*/U_{\text{eq}}$
N1	0.56133 (16)	0.10176 (12)	0.41064 (15)	0.0584 (5)
C11	0.10792 (6)	0.02217 (6)	0.16402 (10)	0.1199 (5)
O2	0.73447 (14)	0.05835 (11)	0.51005 (15)	0.0707 (5)
O3	0.39144 (18)	-0.18904 (14)	0.3085 (2)	0.1148 (9)
O4	0.55981 (16)	-0.20506 (11)	0.42458 (19)	0.0872 (6)
C1	0.63047 (19)	0.04194 (15)	0.44989 (19)	0.0572 (6)
C2	0.60502 (19)	-0.04443 (15)	0.43555 (19)	0.0577 (5)
H2A	0.6582	-0.0845	0.4655	0.069*
C3	0.50216 (18)	-0.06779 (14)	0.37760 (18)	0.0547 (5)
C4	0.42215 (18)	-0.00513 (14)	0.33217 (17)	0.0542 (5)
C5	0.3122 (2)	-0.02093 (17)	0.2719 (2)	0.0645 (6)
H5A	0.2876	-0.0756	0.2569	0.077*
C6	0.2427 (2)	0.04352 (19)	0.2358 (2)	0.0741 (7)
C7	0.2757 (2)	0.12657 (19)	0.2548 (2)	0.0759 (7)
H7A	0.2264	0.1697	0.2294	0.091*
C8	0.3812 (2)	0.14362 (16)	0.3112 (2)	0.0682 (7)
H8A	0.4037	0.1989	0.3233	0.082*
C9	0.45660 (19)	0.07928 (14)	0.35138 (18)	0.0554 (5)
C10	0.7649 (2)	0.14510 (18)	0.5310 (2)	0.0761 (8)
H10A	0.7270	0.1724	0.5651	0.091*
H10B	0.7486	0.1737	0.4629	0.091*
C11	0.8808 (3)	0.1471 (2)	0.6056 (4)	0.1162 (14)
H11A	0.9045	0.2041	0.6195	0.174*
H11B	0.9172	0.1183	0.5720	0.174*
H11C	0.8957	0.1203	0.6736	0.174*
C12	0.4759 (2)	-0.15957 (16)	0.3647 (2)	0.0649 (6)
C13	0.5438 (3)	-0.29493 (18)	0.4194 (4)	0.1060 (12)
H13A	0.4951	-0.3092	0.4477	0.127*
H13B	0.5133	-0.3135	0.3437	0.127*
C14	0.6421 (3)	-0.3350 (2)	0.4822 (6)	0.181 (3)
H14A	0.6739	-0.3139	0.5559	0.271*
H14B	0.6882	-0.3243	0.4503	0.271*
H14C	0.6311	-0.3941	0.4830	0.271*

Atomic displacement parameters (\AA^2)

	U^{11}	U^{22}	U^{33}	U^{12}	U^{13}	U^{23}
N1	0.0598 (11)	0.0493 (10)	0.0607 (11)	-0.0024 (8)	0.0234 (9)	0.0043 (8)
C11	0.0539 (4)	0.0945 (7)	0.1717 (10)	0.0034 (4)	0.0193 (5)	0.0156 (6)
O2	0.0549 (10)	0.0585 (10)	0.0825 (11)	-0.0052 (8)	0.0183 (9)	0.0045 (8)
O3	0.0763 (14)	0.0587 (12)	0.152 (2)	-0.0105 (10)	0.0054 (14)	-0.0116 (13)
O4	0.0709 (12)	0.0473 (10)	0.1220 (16)	0.0002 (8)	0.0268 (11)	0.0063 (10)
C1	0.0556 (13)	0.0541 (12)	0.0576 (12)	-0.0060 (10)	0.0227 (10)	0.0019 (10)
C2	0.0561 (13)	0.0517 (12)	0.0624 (13)	0.0011 (10)	0.0251 (11)	0.0036 (10)
C3	0.0592 (13)	0.0486 (12)	0.0561 (12)	-0.0037 (10)	0.0267 (10)	-0.0002 (9)
C4	0.0579 (13)	0.0540 (12)	0.0509 (11)	-0.0003 (10)	0.0255 (10)	0.0019 (9)
C5	0.0572 (14)	0.0617 (14)	0.0696 (15)	-0.0041 (11)	0.0253 (12)	-0.0001 (11)
C6	0.0533 (14)	0.0739 (17)	0.0837 (18)	0.0037 (12)	0.0223 (13)	0.0067 (14)
C7	0.0659 (16)	0.0661 (16)	0.0890 (19)	0.0116 (13)	0.0303 (14)	0.0087 (14)
C8	0.0661 (15)	0.0539 (13)	0.0782 (16)	0.0041 (11)	0.0283 (13)	0.0067 (12)
C9	0.0586 (13)	0.0519 (12)	0.0543 (12)	-0.0009 (10)	0.0251 (10)	0.0032 (9)
C10	0.0634 (15)	0.0614 (15)	0.0877 (18)	-0.0145 (12)	0.0218 (14)	-0.0014 (13)
C11	0.068 (2)	0.097 (3)	0.140 (3)	-0.0215 (18)	0.012 (2)	0.009 (2)
C12	0.0628 (15)	0.0534 (13)	0.0731 (15)	-0.0026 (11)	0.0272 (12)	-0.0030 (11)
C13	0.100 (2)	0.0447 (15)	0.152 (3)	-0.0038 (15)	0.041 (2)	0.0042 (17)
C14	0.084 (3)	0.057 (2)	0.328 (8)	0.0106 (18)	0.034 (4)	0.033 (3)

Geometric parameters (\AA , $^\circ$)

N1—C1	1.298 (3)	C6—C7	1.394 (4)
N1—C9	1.375 (3)	C7—C8	1.361 (4)
C11—C6	1.737 (3)	C7—H7A	0.9300
O2—C1	1.346 (3)	C8—C9	1.404 (3)
O2—C10	1.444 (3)	C8—H8A	0.9300
O3—C12	1.186 (3)	C10—C11	1.486 (4)
O4—C12	1.313 (3)	C10—H10A	0.9700
O4—C13	1.454 (3)	C10—H10B	0.9700
C1—C2	1.420 (3)	C11—H11A	0.9600
C2—C3	1.356 (3)	C11—H11B	0.9600
C2—H2A	0.9300	C11—H11C	0.9600
C3—C4	1.427 (3)	C13—C14	1.413 (5)
C3—C12	1.506 (3)	C13—H13A	0.9700
C4—C5	1.415 (3)	C13—H13B	0.9700
C4—C9	1.420 (3)	C14—H14A	0.9600
C5—C6	1.355 (4)	C14—H14B	0.9600
C5—H5A	0.9300	C14—H14C	0.9600
C1—N1—C9	117.3 (2)	C8—C9—C4	119.3 (2)
C1—O2—C10	117.0 (2)	O2—C10—C11	107.1 (2)
C12—O4—C13	116.2 (2)	O2—C10—H10A	110.3
N1—C1—O2	121.2 (2)	C11—C10—H10A	110.3
N1—C1—C2	124.4 (2)	O2—C10—H10B	110.3

O2—C1—C2	114.4 (2)	C11—C10—H10B	110.3
C3—C2—C1	119.1 (2)	H10A—C10—H10B	108.6
C3—C2—H2A	120.4	C10—C11—H11A	109.5
C1—C2—H2A	120.4	C10—C11—H11B	109.5
C2—C3—C4	119.3 (2)	H11A—C11—H11B	109.5
C2—C3—C12	118.7 (2)	C10—C11—H11C	109.5
C4—C3—C12	122.0 (2)	H11A—C11—H11C	109.5
C5—C4—C9	118.2 (2)	H11B—C11—H11C	109.5
C5—C4—C3	125.0 (2)	O3—C12—O4	122.8 (3)
C9—C4—C3	116.8 (2)	O3—C12—C3	125.9 (3)
C6—C5—C4	120.1 (2)	O4—C12—C3	111.3 (2)
C6—C5—H5A	120.0	C14—C13—O4	109.3 (3)
C4—C5—H5A	120.0	C14—C13—H13A	109.8
C5—C6—C7	122.1 (3)	O4—C13—H13A	109.8
C5—C6—C11	119.0 (2)	C14—C13—H13B	109.8
C7—C6—C11	118.8 (2)	O4—C13—H13B	109.8
C8—C7—C6	119.0 (3)	H13A—C13—H13B	108.3
C8—C7—H7A	120.5	C13—C14—H14A	109.5
C6—C7—H7A	120.5	C13—C14—H14B	109.5
C7—C8—C9	121.2 (3)	H14A—C14—H14B	109.5
C7—C8—H8A	119.4	C13—C14—H14C	109.5
C9—C8—H8A	119.4	H14A—C14—H14C	109.5
N1—C9—C8	117.6 (2)	H14B—C14—H14C	109.5
N1—C9—C4	123.1 (2)		
C9—N1—C1—O2	-179.1 (2)	C6—C7—C8—C9	-0.8 (4)
C9—N1—C1—C2	0.1 (3)	C1—N1—C9—C8	178.3 (2)
C10—O2—C1—N1	1.5 (3)	C1—N1—C9—C4	0.1 (3)
C10—O2—C1—C2	-177.7 (2)	C7—C8—C9—N1	-177.9 (2)
N1—C1—C2—C3	-0.2 (4)	C7—C8—C9—C4	0.4 (4)
O2—C1—C2—C3	179.0 (2)	C5—C4—C9—N1	178.8 (2)
C1—C2—C3—C4	0.2 (3)	C3—C4—C9—N1	-0.1 (3)
C1—C2—C3—C12	-178.9 (2)	C5—C4—C9—C8	0.6 (3)
C2—C3—C4—C5	-178.9 (2)	C3—C4—C9—C8	-178.3 (2)
C12—C3—C4—C5	0.2 (4)	C1—O2—C10—C11	175.5 (3)
C2—C3—C4—C9	-0.1 (3)	C13—O4—C12—O3	-0.4 (5)
C12—C3—C4—C9	179.0 (2)	C13—O4—C12—C3	179.5 (3)
C9—C4—C5—C6	-1.2 (4)	C2—C3—C12—O3	-172.8 (3)
C3—C4—C5—C6	177.5 (2)	C4—C3—C12—O3	8.1 (4)
C4—C5—C6—C7	0.9 (4)	C2—C3—C12—O4	7.3 (3)
C4—C5—C6—C11	-178.9 (2)	C4—C3—C12—O4	-171.8 (2)
C5—C6—C7—C8	0.1 (5)	C12—O4—C13—C14	176.2 (4)
C11—C6—C7—C8	179.9 (2)		

Hydrogen-bond geometry (Å, °)

D—H···A	D—H	H···A	D···A	D—H···A
C5—H5A···O3	0.93	2.24	2.872 (4)	125